DUCTILITY AND MICROSTRUCTURE OF FERRITIC CAST IRON WITH NODULAR GRAPHITE

D. Aurich, R. Helms and Ch. Zaminer*)

The macroscopic mechanical properties of cast iron with nodular graphite are deeply influenced by the internal microscopic notch effect of the graphite particles and the micro-segregations; this applies to the materials ductility, too. Ductility is quantitatively attributed to internal notch effects which have been evaluated on the basis of a well known relationship between stress and strain concentration and equal matrix properties for the total lot of specimen.

INTRODUCTION

Cast iron with nodular graphite is today an important material for engineering. Due to its substantial ductility the grade GGG 40 is preferentially used with success for heavy section castings and for structures with special requirements (1,2). Ductility as well as Charpy impact energy, mainly the ductility influenced one of the "upper shelf", are considerably lower than that of steel, which is a result of the special microstructure of this cast material. Beyond that it is a suitable model for a rough two-phase material to study the effect of internal notches inside a more or less homogenious (ferritic) steel matrix on strength and ductility.

There are already available valuable reports about strength, ductility and mainly about fracture toughness properties of several nodular iron grades (e.g. 3,4,5,6). In this paper emphasis is laid on the interrelationship between microstructure and basic ductility properties under the influence of tensile deformation.

INTERNAL NOTCH EFFECTS

Based on early considerations about grey cast iron with lamellar graphite there are many attempts to evaluate or to describe the internal notch effect of the graphite particles. These internal notch effects together with a reduction of the load bearing cross section by the inclusions result in a decrease of the modulus of

*) Fed. Institute for Materials Testing, Berlin, Fed.Rep. Germany

elasticity E_o *) , yield limit R_e resp. $R_{p0.2}$, ultimate tensile strength R_m and fracture elongation A_5 or fracture reduction Z. The graphite particles are not load bearing under tensile load and therefore widening with plastic strains, resulting in an increasing global decrease of density.

Out of the various quantities used to describe the internal graphite effects only one should be mentioned (7,8,9):

$$m = \frac{1 - E_o'}{1 - \varrho_o'} \qquad \ldots\ldots\ldots\ldots\ldots\ldots\ldots\ldots (1)$$

where $E_o' = E_o / E_{steel}$ and $\varrho_o' = \varrho_o / \varrho_{steel}$ are the initial moduls resp. the density related to the values of the inclusion free matrix (steel). It is suggested that both - contents and notch effects of the graphite particles - are taken into consideration in the value m. Further investigations show that strength and ductility properties of lamellar as well as nodular iron may be well described by m (7,8,9). Further is shown that m also represents the stress concentration K of a notch, which simulates the total internal notch effects (8).

STRESS AND STRAIN CONCENTRATION

For arbitrary nonlinear stress-strain laws and generalized for arbitrary loading states Neuber (10) proposed a relationship for sharply curved notches between stress and strain concentration factors $K_\sigma = \sigma_{max} / \sigma_n$ resp. $K_\varepsilon = \varepsilon_{max} / \varepsilon_n$

$$\sqrt{K_\sigma \cdot K_\varepsilon} = K_t \qquad \ldots\ldots\ldots\ldots\ldots\ldots\ldots\ldots (2)$$

with K_t Hookian stress concentration factor (linear elastic material). Similar to a proposal of Weiss (11) eq. (2) can be combined with a representation of the materials flow curve, e.g. by the Ramberg-Osgood equation:

$$\frac{\varepsilon}{\varepsilon_o} = \alpha \left(\frac{\sigma}{\sigma_o} \right)^N \qquad \ldots\ldots\ldots\ldots\ldots\ldots\ldots\ldots (3)$$

which results in

$$\sigma_n = \sigma_{max} \cdot K_t^{-2/(1+N)} \qquad \ldots\ldots\ldots\ldots\ldots\ldots (4)$$

$$\varepsilon_n = \varepsilon_{max} \cdot K_t^{-2N/(1+N)} \qquad \ldots\ldots\ldots\ldots\ldots\ldots (5)$$

the relationship between max. stress resp. strain in the notch root (index max) and the nominal values (index n). For a fracture mechanism due to a critical local stress $\sigma_{max} = \sigma_f$ eq. (4) has to be applied, and for a more ductile mechanism due to a critical local strain $\varepsilon_{max} = \varepsilon_f$ eq.(5) should give the proper assessment. For further considerations eq.(4) and (5) can be combined:

$$\frac{\sigma_n}{\varepsilon_n} = \frac{\sigma_{max}}{\varepsilon_{max}} \cdot K_t^{2(N-1)/(1+N)} \qquad \ldots\ldots\ldots\ldots\ldots\ldots (6)$$

*) Index o: at very low stress

If σ_{max} is substituted by ε_{max} with the aid of eq.(3) it can be found

$$\frac{\sigma_o}{\sigma_n} = \frac{1}{\varepsilon_n} (\alpha \varepsilon_o)^{1/N} \cdot \varepsilon_{max}^{(N-1)/N} \cdot K_t^{-2(N-1)/(1+N)} \quad \ldots\ldots\ldots\ldots (7)$$

TEST MATERIAL

143 tensile specimens of 14 mm diameter were taken from two annealed (48 h at 740 °C) test castings of the dimensions 40 x 40 x 120 cm with a modulus of approx. 9 cm.

The approx. homogenious chemical composition, the microstructure and the attributed ductility of seven specimens selected out of the total lot and representing a wide range of the ductility (expressed by Z) of the material are given in table 1 and 2. Very different mechanical properties - mainly the ductility - are obtained related to the respective position of the specimen inside of the test castings and thus to the respective cooling condition. It is remarkable that the present graphite distribution is relative coarse and beyond that separated in two generations: large primary graphite nodules precipitated from the melt and smaller secondary nodules generated during ferritising heat treatment. It is suggested that the ductility will be mainly influenced by the existence of a few graphite nodules with a low degree of spherodization and/or by micro-segregation (of the melt) including lamellar graphite.

TABLE 1 — Chemical Composition in Mass - %

C	Si	Mn	P	S	Cu	Ni	Mg
3.26...	1.90...	0.19...	0.010...	0.004...	0.044...	1.01...	0.049...
3.49	1.94	0.20	0.016	0.007	0.049	1.04	0.058

TEST RESULTS

It is obvious from table 2 that - with the exception of low ductility material - the fracture surfaces throughout point out a ductile fracture mechanism by the formation of dimples at the graphite nodules. Related to the very low ductility ($Z \leq 4$ %) it is not yet clear wether an incipient dimple mechanism is interrupted by cleavage fracture formation or cleavage fracture portions after small plasticization are arrested by voids at the graphite nodules.

The total amount of test results is summarized in figures 1 and 2 as plots of the mean values of the yield (proof) stress $R_{p0.2}$ and the true fracture stress R_f vs. ductility respective $R_{p0.2}/R_f$ vs. ductility; the reduction of area at fracture Z is used as ductility. The true fracture stress can be evaluated with sufficient accuracy by

$$R_f \approx \frac{R_m}{1-Z} \quad , \quad Z \leq 20\ \% \quad , \quad \ldots\ldots\ldots\ldots\ldots\ldots (8)$$

with $R_m = F_{max}/S_o$ the ultimate tensile stress, because it is observed, that this material shows a slight necking and load drop in the high ductility range only (Z>20%). Based on the assumption that the matrix properties are comparable for all specimen, which is confirmed by the approx. constant yield stress $R_{p0.2}$, eq. (7) can be applied to quantify the internal notch effects by adapting it to the experimental results plotted in figure 2.

TABLE 2 - Microstructure and Ductility of 7 Representative Specimens

Ductility Z	Matrix: Ferrite grain size 1)	Matrix: Perlite	Graphite: Type of graphite 3) 4)	Graphite: Diameter 1) 5) prim.	Graphite: Diameter 1) 5) sec.	Graphite: Number total: prim. and sec.	Graphite: Distance total: prim. and sec.	Fracture surface: Cleavage	Fracture surface: Dimples
%	µm	Vol.-%		µm	µm	mm^{-2}	µm	%	%
2	2)	8	V(IV-III)	128		14	576	45	55
4	2)	4	V(IV-III)	128		12	601	25	75
7	47	4	V(IV-III)	119	0	15	501	-	100
12	46	3	V	82	to	27	383	8	92
17	55	3	VI (V)	70	35	28	365	-	100
20	42	4	VI (V)	63		25	380	-	100
22	50	2	VI	59		53	278	-	100

1) Mean values
2) Subgrains
3) According to ISO/R 945-1969(E)
4) Sporadical graphite types in brackets
5) Diameter of the equivalent area circle

For that purpose eq. (7) may be applied with the constant stress $\sigma_o = R_{p0.2} = 268$ N/mm² and $\varepsilon_o = R_{p0.2}/E + 0.002 = 0.0038$ (E = 150 000 N/mm²) as well as with the constants $\alpha = 5.5$ and N = 4.2 of the Ramberg-Osgood representation of the flow curve for $\varepsilon > 3\%$ (figure 1). For the instant of fracture is $\sigma_{nf} = R_f$; $\varepsilon_{nf} = Z/(1-Z)$ and furthermore ε_{max} is the ductility of the matrix, supposed to be constant ($\varepsilon_{max} = C$) under the above mentioned conditions.

$$\frac{R_{p0.2}}{R_f} = 0.398 \cdot C^{0.762} \cdot \frac{1-Z}{Z} \cdot K_t^{-1.231} \qquad \ldots\ldots\ldots\ldots\ldots\ldots (9)$$

may then be derived from eq. (7).

Based on figure 2 it is plausible to adapt the notch effect of optimal graphite nodules (t/r = 1) with a theoretical Hookian stress concentration factor $K_t = 2$ (12,13) to a higher ductility (e.g. Z = 20%). For this combination a matrix ductility C = 0,78 can be evaluated from eq. (9). Then adapting the test results of figure 2 to eq.(9) K_t-values up to 8.6 added in figure 2 seem to be effective with respect to a reduction of the ductility at least in the range Z > 4%.

DISCUSSION

The level of the number of graphite nodules seems to have no predominant influence; in spite of the coarse distribution (max.53 mm^{-2}) high ductility ($Z > 20\%$) is partly attained in the present case. - Decreasing ductility due to increasing internal notch effect is therefore attributed to the following details:

a. Deviation of at least some if the graphite nodules or other inclusions from the ideal spherical shape (12,13). K_t-values of approx. 8 may be attributed to very flat internal notches of $t/r \approx 30$ (12).

b. Increasing stress interference with decreasing relative nodule distances d/t (14). At $d/t \approx 7.5$ practically no more interference is expected (14).

c. Additional stress concentration is expected for internal notches near the free surface of the tensile specimen (15).

At the time being it is difficult to separate the above mentioned points with regard to their contribution to internal notch effects or to quantify internal notches by the geometrical dimensions only with sufficient accuracy. Notwithstanding that an attempt was made to evaluate the Hookian stress concentration factors K_t (12) for the most crucial graphite noduls and micro-segregations from polished sections attributed to different ductility. From figure 3 it may be concluded that in the present case

- the ductility is mainly influenced by the internal notches of the micro-segregations. Their K_t-values, evaluated from the segregation geometry, coincide better with those evaluated by the test results applying eq.(9);

- for low ductility the internal notch effect is underestimated, for high ductility overestimated by the micro-segregation geometry, which gives hints to a possible additional influence of the matrix ductility.

SYMBOLS USED

C	= matrix ductility
d	= inclusion distance; spacing (mm)
E	= modulus of elasticity (N/mm^2)
K_ε	= strain concentration factor
K_σ	= stress concentration factor
K_t	= Hookian stress concentration factor
m	= characteristic value for cast iron
N	= constant in the Ramberg-Osgood representation
r	= small radius of an elliptical particle (mm)
$R_{p0.2}$	= yield limit (N/mm^2)

R_m = ultimate tensile strength (N/mm^2)

R_f = true fracture stress (N/mm^2)

t = half particle width (mm)

Z = reduction of area at fracture

α = constant in the Ramberg-Osgood representation

ε = engineering strain

σ = stress (N/mm^2)

σ_o, ε_o = normalizing values in the Ramberg-Osgood representation (N/mm^2 resp. %)

ρ = density (g/cm^3)

REFERENCES

1. Motz; J.M., 1980, "Fracture mechanical properties in heavy sections of ferritic nodular iron castings", Proc. 6th Intern.Symp.PATRAM, Vol.1, 655, Berlin (West),Germany
2. Methling, D., Treffner, F.J. and Schilling, F., 1980, "Production of castor casks for the transportation and storage of spent fuel element bundles - management and quality assurance", Proc. 6th Intern. Symp. PATRAM, Vol. 1, 682, Berlin (West), Germany.
3. Motz, J.M., 1980, Gießerei, 67, 682
4. Motz, J.M. et al. 1980, Gießereiforschung, 32, 97
5. Jolley, G. and Holdsworth, S.R., 1977, "Ductile fracture initiation and propagation in ferritic s.g. cast iron", Proc. 4th Intern. Conf. Fracture, Vol. 2, 403, Waterloo, Canada.
6. Hornbogen, E. and Motz, J.M. 1977, Gießereiforschung, 29, 115.
7. Pohl, D., 1967, Gießereiforschung, 19, 191.
8. Pohl, D., 1971, Gießereiforschung, 23, 159.
9. Pohl, D., 1977, Gießerei, 64, 629.
10. Neuber, H., 1961, Trans. ASME, 28E, 544.
11. Weiss, V., 1971, Schweizer Archiv, 37,41.
12. Neuber, H., 1958, Kerbspannungslehre, 2. Auflage, Berlin.
13. Sadowsky, M.A. and Sternberg, E., 1949, J. appl.Mech., 16 149.
14. Sternberg, E. and Sadowsky, M.A., 1952, J. appl. Mech., 19,19.
15. Hanus, J.B. and Burger, C.P., 1981, Experimental Mechanics, 336.

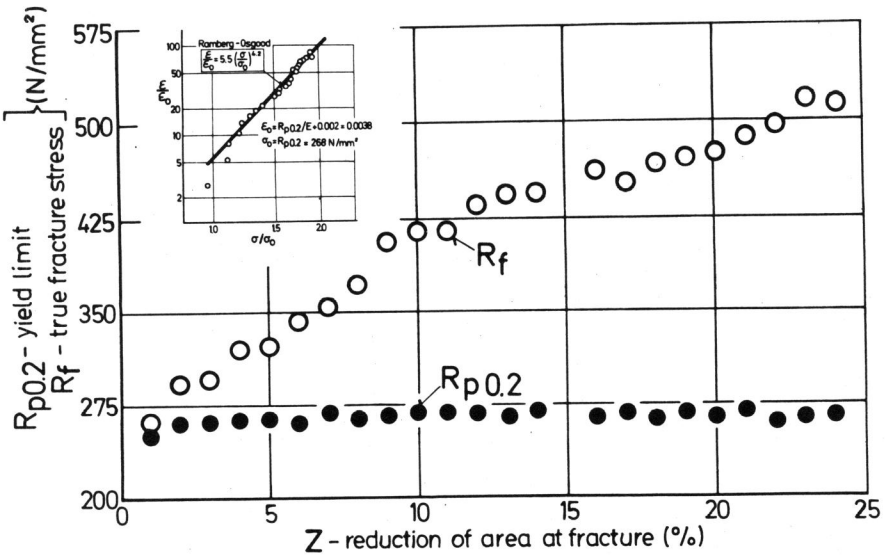

Figure 1 Yield limit and true fracture stress vs. ductility; mean values.

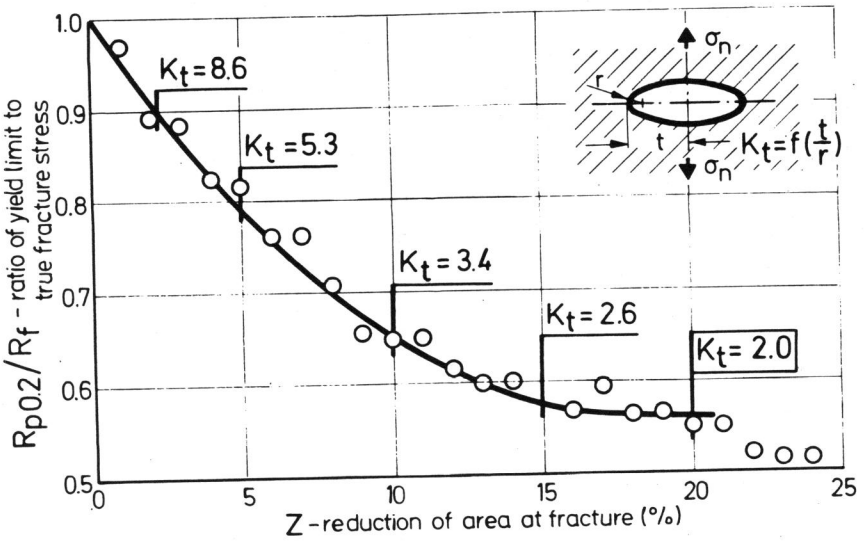

Figure 2 Yield limit related to true fracture stress vs. ductility; attributed effective internal notch effect.

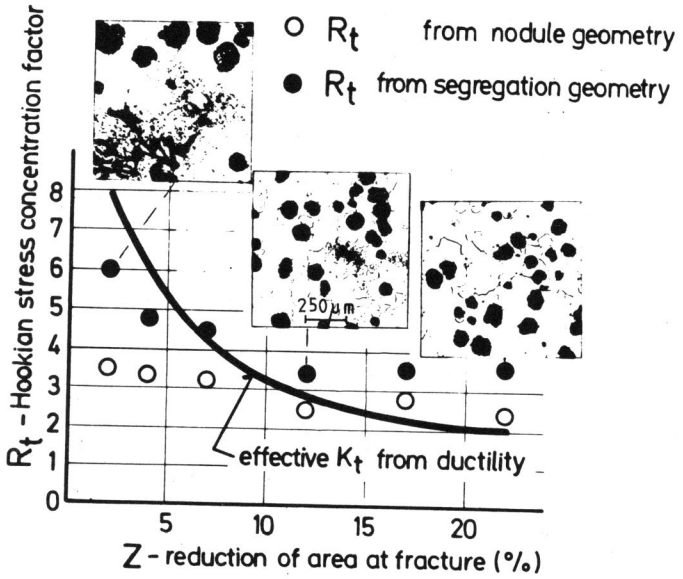

Figure 3 Internal notch effect evaluated from inclusion geometry compared with effective K_t-values.